The Tropical Warm Pool International Cloud Experiment (TWP ICE)

Peter T. May[1], James H. Mather[2], Geraint Vaughan[3], Christian Jakob[1], Greg M. McFarquhar[4], Keith N. Bower[3], and Gerald G. Mace[5]

1 Bureau of Meteorology Research Centre, Melbourne, Australia

2. Pacific Northwest National Laboratory, Richland, Washington, USA

3. School of Earth, Atmospheric and Environmental Sciences, University of Manchester, UK

4. Department of Atmospheric Sciences, University of Illinois, Illinois, USA

5. Meteorology Department, University of Utah, Utah, USA

Abstract

One of the most comprehensive data sets of tropical cloud systems and their environmental setting and impacts ever sampled has been collected during the Tropical Warm Pool International Cloud Experiment (TWP-ICE) and ACTIVE (Aerosol and Chemical Transport In tropical conVEction) campaign in the area around Darwin, Northern Australia in January and February of 2006. The experiment design utilized permanent observational facilities in Darwin which include a polarimetric weather radar operated by the Australia Bureau of Meteorology and a suite of cloud remote sensing instruments operated by the US Department of Energy (DOE) Atmospheric Radiation Measurement (ARM) program. A dense network of observational systems added for the experiment included sea-soar and buoys for ocean observations, cloud radars, wind profilers, radiation measurements, two AERI's, a lightning network and a six site balloon-borne sounding network. A fleet of five research aircraft were deployed including two high altitude aircraft for characterizing cloud properties and the atmospheric state, a plane carrying airborne cloud radar and lidar and two aircraft sampling the boundary layer in great detail including fluxes, aerosols and chemistry. An integral factor in the experiment design was to provide boundary conditions and validation data sets for a range of modelling activities and cloud retrieval development.

1. Introduction

A crucial factor for our ability to forecast future climate change is a better representation of tropical convection and clouds in climate models. This requires a better understanding of the multi-scale factors that control tropical convection as well as an improved understanding of how the characteristics of the convection affect the density and nature of the cloud particles that are found in deep convective anvils and tropical cirrus. Deep convection also lifts boundary-layer air into the Tropical Tropopause Layer (TTL), affecting the composition of this region and through it the global stratosphere. Understanding the transport of gases and particles in deep convection is also therefore of global importance. As a response to this challenge, a major field experiment named the Tropical Warm Pool International Cloud Experiment (TWP-ICE), including the UK ACTIVE (Aerosol and Chemical Transport In tropical conVEction) consortium, was undertaken in the Darwin, Northern Australia area in January and February 2006. The overall goals of the experiment were to observe the evolution of the cloud systems, their environmental controls and their impacts from the initial convective cells through to the decaying and self-maintaining cirrus, including their impact on upper tropospheric composition. TWP-ICE builds on such experiments as the Tropical Ocean Global Atmosphere Coupled Ocean Atmosphere Response experiment (TOGA-COARE; Webster and Lukas, 1992) and the Central Equatorial Pacific Ocean Experiment (CEPEX; http://www-c4.ucsd.edu/cepex; Heymsfield and McFarquhar, 1996) that focused on air-sea interactions along with their impact on convection and convectively generated cirrus

respectively. Cloud sampling strategies employed during TWP-ICE built on previous experiments such as the Cirrus Regional Study of Tropical Anvils and Cirrus Layers - Florida Area Cirrus Experiment (CRYSTAL-FACE; Garrett et al., 2005; Heymsfield et al., 2005) which emphasized the physical and chemical properties of cirrus and the upper troposphere region.

The experiment was designed to provide a comprehensive data set for the development of cloud remote sensing retrievals and initialising and verifying a range of process-scale models, with a view to improving the parameterisation of tropical convection and clouds in numerical weather prediction and climate models. Accordingly, a surface measurement network (including a research ship) of unprecedented coverage for a tropical experiment was combined with a fleet of five research aircraft to enable in-situ and remote-sensing measurements of clouds, meteorological variables and composition from the ground into the lower stratosphere.

A major motivation for choosing the Darwin area as the experiment location is that it samples a wide variety of convective systems, including those typical for a monsoon coastal environment, similar to those experienced by large populations under the influence of the Asian and Indian monsoons. Monsoon cloud systems are typically oceanic and the lessons of TWPICE will be applied across tropical oceanic areas including the InterTropical Convergence Zone (ITCZ). The monsoon has very high intra-seasonal variability (e.g. Drosdowsky, 1996), and experiences both active periods with storms typical of a maritime environment and “breaks” when the storm systems are

characteristic of coastal and continental areas. These break storms have high lightning activity and are often isolated, forming on sea breezes and other local circulations, although some of these ultimately develop into squall lines. This is in contrast to the widespread, but generally weaker convective activity sampled during the active phase of the monsoon (e.g. Mapes and Houze, 1992; Keenan and Carbone, 1992; May and Ballinger, 2007). The TWPICE period sampled both these regimes as well as a relatively suppressed period with storms of only moderate vertical extent.

Another important feature that makes Darwin the ideal site for studying tropical convection is that it boasts what is probably the most comprehensive long term meteorological observational network anywhere in the tropics. This includes research polarimetric radar, Doppler weather radar, wind profilers, a radiosonde station, the Australian Bureau of Meteorology (hereafter, referred to as the Bureau) operational mesonet and the Darwin Atmospheric Radiation Measurement (ARM) Climate Research Facility (ACRF) site operated by the US Department of Energy. These systems all provide long term data sets so that the TWPICE data can be put into a climatological context.

The combination of excellent facilities and the range of tropical weather experienced has made for a long history of field programs in the Darwin area. Important examples of these were the combined AMEX/EMEX/STEP (Australian Monsoon Experiment / Equatorial Monsooon Experiment / Stratopshere-Troposphere Exchange Program) programs in the late 1980s focussing on the structure of the Australian monsoon and the potential impact

on troposphere/stratosphere transport (e.g. Keenan et al., 1989; Mapes and Houze, 1992; Russell et al., 1993), the Maritime Continent Thunderstorm Experiment (MCTEX) focussing on the evolution of intense island based thunderstorms (Keenan et al, 2000), the Darwin Waves Experiment focussing on convectively generated gravity waves (Hamilton et al., 2004) and the Emerald experiment focussing on cirrus measurements around deep intense storms (Whiteway et al, 2004) .

The science goals of the experiment are listed in Table 1. A general theme was to document in as much detail as possible the evolution of the cloud systems, the environmental controls on this evolution and their impact on the environment. Another important component was to provide data for the validation of ground and space borne remotely sensed cloud properties as these tie the experiment into long-term observational data sets in the tropics (e.g Ackerman and Stokes, 2003). The main focus of activities was within a ring of radiosonde stations established around Darwin for the experiment although survey aircraft missions were conducted to measure the large scale aerosol and chemical composition of the region and to sample highly aged cirrus (clouds separated from their parent convection more than 24 hours) when the centre of deep convection was located well to the south.

A key goal of the research being conducted with TWPICE data is to understand the link between the strength and organisation of the parent convection, the properties of the aerosol feeding into the storms, and the resulting cirrus characteristics. Measurements of aerosol size distribution and

composition (including black carbon) were made with both low and high-level aircraft, to enable accurate initialisation of cloud-resolving models and evaluation of their predictions. These measurements followed on from those made by ACTIVE in the pre-Christmas campaign, as described in the companion paper (Vaughan et al 2006), and to document the evolution of the atmosphere from one with substantial impact from biomass burning at the end of the dry season to pristine conditions in late January.

2. Ground Network Observations

One of the cornerstones of TWP-ICE was an extensive ground-based observational network that included long-term components as well as instruments deployed specifically for the campaign. The network spanned a region with a radius of approximately 150 km, centred on Darwin. The long-term component included Bureau instrumentation associated with both meteorological research and operational forecasting applications (Keenan and Manton, 1996), as well as a DOE Atmospheric Cloud and Radiation Facility (ACRF) site (Ackerman and Stokes, 2003). Additional instrumentation deployed for the campaign included a network of radiosonde sites, surface energy flux systems, radar wind and cloud profilers, multichannel microwave instruments, two AERIs, ocean observations and a lightning detection network. Figure 1 illustrates the TWP-ICE/ACTIVE campaign region including the location of some of these observation elements. This instrument network served multiple purposes: it provided detailed information about the

meteorological environment which was critical for mission flight planning and will be important for measurement interpretation; it provided detailed information about the vertical distribution of cloud properties, a major focus of the campaign; and it provided boundary conditions for the experiment domain to aid in post-experiment model simulations of the campaign.

The Bureau operates an extensive suite of instrumentation in the Darwin region. Bureau observation assets in this region are listed in Table 2. These include two weather radar systems, a radiosonde launch site, wind profilers and a network of Automated Weather Stations (AWS). These instruments provide a long-term baseline for meteorological conditions in the Darwin region and a detailed description of the region during the campaign. Of particular interest for the experiment are the two weather radars. One is fully polarimetric (Keenan et al., 1998) and the other is an operational Doppler system. They have a baseline of approximately 25 km and have a dual-Doppler lobe over the open ocean. This combination allows the three dimensional wind field to be measured within the precipitation and thicker cloud regions of the convective systems. Both radars complete a volume scan every 10 minutes, allowing the evolution of the anvils within complex convective systems to be followed. Thus they provide key observations for the interpretation of other measurements. With 3-D radar reflectivity images available to the science team in real time, they were also crucial for directing the aircraft toward regions of interest and away from convective turrets. The polarimetric radar also provides a classification of the microphysical habit of hydrometeors detected by the radar (Keenan 2003; May and Keenan, 2005).

While the Bureau scanning radars provided information about the three-dimensional distribution of convective clouds, a lightning network was deployed by DLR specifically for the experiment period (e.g. Betz et al, 2004). Lightning activity provides additional information about convective intensity and the microphysical processes going on in the convective cores.

Since 2002, ARM has operated an atmospheric radiation and cloud observing site in Darwin. This is the third ARM site to be deployed in the tropics after the sites at Manus Island (Papua New Guinea) and Nauru (Mather et al., 1998). The tropical ARM sites include measurements of the surface radiation budget, surface meteorology and the vertical distribution of clouds (Table 2). Cloud profiles are derived primarily from a pair of vertically-pointing active remote sensors: a 35 GHz cloud radar and a cloud lidar (Clothiaux et al., 2000). In addition to cloud occurrence, these instruments provide profiles of cloud microphysical properties through various retrieval algorithms (eg., Hogan et al., 2000; Mather et al., 2006). A goal of TWP-ICE is to use in-situ observations of microphysical properties to improve the retrieval of these properties from the long-term ground-based remote sensors at Darwin and the other tropical ARM sites. Several other profiling instruments were located at and near the Darwin ARM site and elsewhere (Table 3) for the TWP-ICE campaign, including a 50 MHz radar (Vincent et al, 1998), a 2.8 GHz radar (Ecklund et al., 1999) and a passive microwave radiometer (HATPRO: Westwater et al., 2005)

As mentioned above, another goal of TWP-ICE was to provide the necessary boundary conditions so that meteorological simulations can be run for the experiment period. Of particular interest are high-resolution models that capture the details of convection and cirrus production, as well as single column models that are key tools for climate model parameterisation development. The observations from the Bureau and ARM radars then provide the means of evaluating the modelled cloud fields. The lateral boundary conditions are provided by a network of five radiosonde sites (Figure 1) from which balloons carrying Vaisala RS-92 radiosondes were launched at 3-hourly intervals for the experiment period as well as 6-hourly soundings from the central facility. The data from these individual profiles will be integrated into an analysis of the large-scale dynamical forcing (Zhang et al., 2001). This forcing data set also makes use of measurements of the upper and lower boundary conditions in the experiment domain, such as the regional precipitation derived from the Bureau polarimetric radar, surface energy fluxes, and top-of-the-atmosphere and surface radiative fluxes. In support of this activity stations measuring sensible and latent heat fluxes as well as radiative fluxes were deployed at several locations throughout the experiment domain chosen to represent a range of representative surface types from open water to savannah (e.g. Beringer and Tapper, 2002). Top of the atmosphere boundary conditions are provided by satellites including the new Japanese geostationary satellite, MTSAT-1R and various polar orbiting platforms. Cloud products associated with multiple satellites have been derived by the NASA Cloud and Radiation Support group (http://www_pm.larc.nasa.gov).

To complement aircraft measurements of TTL composition, a programme of ozonesonde launches was conducted from Darwin during the ACTIVE campaign. Most of these were launched in November and December, because of the greater focus on TTL composition compared to cloud measurements in that period (Vaughan et al 2006), but five were also launched during TWP-ICE. They showed a progression from a uniformly low ozone concentration (20 ppbv) during the active monsoon in mid-January to profiles similar to the pre-monsoon period in mid-February, with maximum ozone mixing ratio up to 60 ppbv in the mid-troposphere and a minimum < 20 ppbv in the TTL.

Darwin is a coastal site, which means that a significant part of the experiment domain was over water. Therefore, it was important to characterize the oceanic region off the Australia coast. For this purpose, the Australian National Research Facility Research Vessel Southern Surveyor operated by CSIRO (Commononwealth Scientific and Industrial Research Organisation) was stationed in the Timor Sea west of Darwin. This ship served as the base for multiple observations: radiosondes were launched to complete the network of sites around the domain perimeter; the ship carried instruments for measuring turbulent and radiative fluxes (e.g. Fairall et al., 2003); a second set of cloud remote sensing instruments was used to sample cloud properties away from coastal influences and to provide a second remote sensing comparison target for the aircraft; finally, several instruments were deployed

to measure ocean conductivity/temperature/depth (CTD) and current profiles (Godfrey et al., 1999). These measurements provide an important link between surface fluxes and the ocean mixed layer structure. Miniature CTD probes were mounted on a SEASOAR profiling platform and on three shallow moorings. In addition periodic CTD casts were made during the voyage to compare with the continuous profiles. The combination of cloud observations with frequent soundings, surface and radiative flux measurements as well as sea state will allow the diurnal cycle over the ocean to be examined in detail. Further aims of the ocean observations were to provide measurements of the ocean state to support both ocean and coupled modelling as well as document the impact of the convection on the structure of the upper ocean. The ocean dynamics of the ship operations area can be categorized as somewhere between a coastal sea and the open ocean, where the combination of shallow water (50 m) and strong tides will have some influence on the mixed layer dynamics. The duration of the experiment was also long enough that tidal mixing varied significantly during the observation period. This should allow the model to isolate tidal mixing from other mixing processes such as night-time convection.

3. Aircraft operations

There were five research aircraft deployed for TWPICE (Table 4). Two of these, the Scaled Composite Proteus carrying the ARM-UAV suite of instruments and Airborne Research Australia (ARA) Egrett, were high altitude

aircraft capable of in-situ measurements in the anvil outflow. Their payloads included instruments for detailed microphysical and meteorological measurements, and in the case of the Egrett a suite of chemical and aerosol instrumentation. Details of the Egrett payload may be found in Table 1 of the companion paper (Vaughan et al 2006), but the main features were measurements of cloud and aerosol particle size distribution, cloud particle imaging, fast-response H_2O, CO, O_3, condensation nuclei and NO_x. Detailed but less frequent chemical measurements were taken from an on-board gas chromatograph and an automated tube sampler. An instrument to measure aerosol size distribution and black carbon fraction alternated with a NO_x instrument. A summary of the observations undertaken by the Proteus are listed in Table 4 and a detailed list of instruments are available on the on-line companion tables to this paper. Key instruments on the Proteus included probes for measuring ice particle size distributions, ice water content, and ice crystal habit as well as cloud detection lidar and a suite of solar and infrared passive remote sensors, together with probes measuring state parameters, water vapour and CO and CO_2 concentrations. A third aircraft, a Twin Otter, carried an airborne vertically pointing 95 GHz cloud radar and lidar to support the high-altitude measurements was flown at an altitude of about 3300 m. The remaining two aircraft were dedicated to boundary layer measurements. The Dimona had the capability for turbulent flux measurements and was primarily deployed at very low altitudes except for some missions exploring the effect of convection on boundary layer structure and the recovery of the boundary layer after convection. The UK NERC (Natural Environment Research Council) Dornier aircraft carried an extensive suite of instruments

for aerosol, chemical and state measurements, including a meteorological probe, particle size spectrometers, an aerosol mass spectrometer and fast-response CO, O_3 and NO_x, as well as a similar gas chromatograph and tube sampler to the Egrett. Full details of the Dornier payload may be found in Table 2 of Vaughan et al (2006). This aircraft was deployed for areal surveys as well as probing the boundary layer air being ingested into the storm systems being sampled by the high altitude aircraft.

Table 5 lists the mission goals from the more than 25 missions which were flown ranging from single-aircraft flux inter-comparison flights and surveys to coordinated multi-aircraft missions sampling well-developed deep convective systems. Mission priorities were determined by a decision-making team the evening before a flight, following daily weather briefings. The priorities were re-assessed the following morning and options kept open until flight times.

Aircraft management after takeoff was coordinated through a dedicated flight control centre manned by an experienced team including a former research aircraft pilot. The team had access to a very flexible full four-dimensional radar visualisation system that included flight tracks, hourly geostationary IR and visible imagery as well as an extensive network of surface and sounding data. The radar and satellites were the primary tool for directing aircraft to key locations and maintaining aircraft safety. Feedback from the pilots and science teams on the aircraft was also crucial for the detailed location of flight tracks and altitudes. A variety of means were used to communicate with the aircraft including radio, email, satellite phones and an internet chat room.

There were several classes of mission as outlined in Table 5. There were several multi-aircraft missions directed towards the understanding of the cirrus structure and evolution. Where possible these missions included the Twin Otter flying beneath the high altitude aircraft. In this way, concurrent remote sensing and in situ cloud observations obtained from the aircraft can be used to improve retrievals from long-term ground (ACRF) and satellite (CLOUDSAT/Calipso) based remote sensors. There were two classes of cirrus sampling missions. In one class, the aircraft were directed as close as possible in space and time to fresh anvil clouds to study the microphysics, aerosol and chemistry of the cloud being ejected from the convection and its evolution. The Dornier and Dimona were utilised in these missions to sample the boundary layer structure both ahead of the storms and in the lee. The second class of multi-aircraft missions were aimed at sampling aged cirrus where the internal circulations of the cirrus and new crystal growth was dominant There is a distinct change in crystal habit associated with this transition.

Where possible the Proteus also performed spiral ascents and descents through the clouds over the ground based and ship based remote sensing sites. Again this has a strong link to algorithm development and validation of retrievals from Cloudsat/Calipso and long term records at the ACRF and other sites.

A variety of survey type flights were undertaken in order to examine the properties of the air masses around Darwin and the spatial structure, both of the boundary layer and upper troposphere. These missions were of two basic types – flights in clear air at a number of altitudes in the Darwin area to obtain profile information, and long-range missions at constant altitude. Between 30 January and 3 February the Dornier flew north towards Indonesia and south to Alice Springs in central Australia. At the northern limit of these flights air with much more pollution than in Darwin was encountered, consistent with a northern hemisphere origin. Far less variation was seen on the way to Alice Springs. Two local survey flights of the Egrett as well as one towards Indonesia were also conducted during this period, which coincided with the inactive monsoon (see below).

The final class of mission reflects that one of the factors underpinning model studies and the provision of forcing data sets is an estimate of area averaged surface fluxes. Several ground sites were deployed to address this, but the Dimona was necessary for comparing the sites and gaining estimates of the spatial variability of the fluxes so that the point measurements can be turned into areal averages including some knowledge of the uncertainties in these estimates. These were performed under a variety of cloud cover conditions, but precipitation was avoided to minimise spatial sampling issues.

4. Meteorological conditions

Four distinct convective regimes were sampled during the intense observing period (IOP) of TWP-ICE. These were examples of active monsoon conditions, a relatively suppressed monsoon situation followed by three days of clear skies and then a classic break period[1]. This succession of events was associated with a large-amplitude Madden-Julian Oscillation (MJO) event. A series of figures will be used to illustrate the evolution of the meteorological conditions. Those will be introduced here and referred to throughout this section. Figure 2 shows the time-accumulation of area-averaged rainfall derived from the radar data. It is evident that despite a great variability in convective organisation and the occasional presence of large stratiform areas, each precipitating regime produced a remarkably constant area-averaged rainfall. One singular mesoscale convective system (MCS) stands out in the record because it produced an area-averaged rainfall accumulation of more than 70 mm (Fig. 2).

Figure 3 shows a time-height cross-section of relative humidity measured by radiosondes from Point Stuart (Fig 1). Figure 4 shows the median Convective Available Potential Energy (CAPE) from all sounding sites (see Fig. 1 for their location) together with the area-averaged hourly rainfall throughout the TWP-

[1] There are various definitions of monsoon conditions (e.g. Drosdowsky, 1996), but the principal feature of the monsoon in Darwin is the presence of westerly winds between 850 and 700 hPa. The use of more complex definitions usually only change the "monsoon periods" by a few days. We will largely use a simple definition here of westerlies at 700 hPa in a 2 day smoothed wind time series except where explicitly discussed.

ICE period. Figure 5 shows the vertical distribution of clouds averaged over the three convectively active and one suppressed periods as identified by the mm-cloud radar (MMCR) at the ARM site in Darwin. Figure 6 highlights examples of the cloud and rainfall distribution for each of the three precipitating periods.

At the beginning of the IOP the Darwin area experienced very active monsoon conditions. There was a great variety of convective organisation during this period with isolated storms, as well as lines aligned along, across and at some angle to the shear (or all at once in a single scene). Widely varying amounts of stratiform rain were associated with the various lines. A constant feature during this period was the dense overcast cirrus present across the domain. Outflows from the deep convective storms were mixing with existing aged cirrus so that cirrus sampled during this period was unlikely to be representative of either pristine new or aged anvil cirrus, but rather constituted a mixture of those types except close to the convective towers. As is evident from Figure 2, the area-mean rainfall rates for this period were around 17 mm/day. This period was marked by high values of relative humidity throughout the troposphere (Fig 3) and relatively high values of CAPE (Fig 4). Consistent with the high humidity values, the monsoon period was characterized by a high frequency of occurrence of clouds detected by the MMCR throughout the column, by far the highest values of the TWP-ICE period. As, the example in Figure 6 (left column) shows convection in this period was typically very wide-spread. Individual cells are not of great intensity with high reflectivities rarely extending much above the freezing

level. However, radar echo tops still extended to about 17 km for the most intense cells (see middle row of panels of Figure 6).

By January 24 the monsoon trough was receding to the north of Darwin and easterly winds were being experienced at 700 hPa, although the cloud conditions and storm character were still monsoonal. A large MCS developed in the region, which developed a distinct circulation as it moved across the measurement array towards the sea west of Darwin. The area-averaged rainfall rate during the passage of the MCS was about 70 mm/day (see Fig 2). The soundings immediately before the passage of the system through the experiment area showed the highest CAPE of the monsoon periods covered by TWP-ICE. The system developed into a tropical low and would almost certainly have become a tropical cyclone had it not made landfall to the southwest of Darwin at a central pressure of 999 hPa. The system continued to intensify, eventually deepening to 988 hPa over the land on January 31. It established itself as an almost stationary feature over the central part of the Northern Territory until February 2. It was sufficiently intense and had a spiral cloud structure such that it was informally dubbed “Landphoon John”. Widespread deep convection and torrential rain associated with this low brought extensive flooding to the semi-arid lands south of Darwin.

The presence of this cyclonic centre to the south had several impacts on the cloud systems around Darwin. Its circulation sustained surface westerly winds of more than 20 ms^{-1} across the Darwin area and adjacent waters, but also advected very dry continental air over the experimental area at mid-levels

(Fig 3). This had the effect of limiting storm heights during this period to below about 8-10 km. The organisation ranged from isolated cells to short lines, but with no significant stratiform cloud. While CAPE remained high (Fig 4), the limiting effect of the dry mid-troposphere on convective cloud depth led to significantly lower rain rates of about 5-7 mm/day. The vertical cloud distribution during this period shows two distinct peaks in the lower and upper troposphere (yellow line, Fig 5). The higher maximum was due to strong advection of cirrus northward from the cyclone centre to the south. The snapshots in Figure 6 (middle column) show the large area with low brightness temperature to the south of the Darwin area with cirrus bands emanating from this area. Most of the experiment area was covered by relatively low-level clouds. The radar images indicate mostly shallow rain features, although individual small cells reaching the 10 km level were regularly observed. Darwin experienced the cleanest low-level air measured during the campaign - < 50 ppbv of CO and less than 1 aerosol particle per cm^3 in the size range > 300 nm diameter.

The low dissipated rapidly on February 3 and three days of clear skies and no precipitation was experienced. These days were associated with the lowest CAPE throughout the experiment (Fig 4) and showed the driest conditions above the boundary layer measured in TWP-ICE (Fig 3). Consistent with these conditions the cloud radar observed hardly any cloud (green line of Fig 5).

With the dissipation of the intense low to the south conditions in the experiment area changed to those typical for a monsoon break with easterly flow throughout the column. As is typical, convection during this period exhibited intense afternoon thunderstorms, but also several squall lines passing Darwin in the evening and early morning. These lines had their genesis in the previous afternoon's convection to the east. Despite the great intensity of these convective systems, area-mean rainfall during this period was only around 8 mm/day due to their relatively small coverage (in space and time) compared to the monsoon conditions (Fig 2). The period was accompanied by a gradual moistening of the middle and upper troposphere (Fig 3) and gradual increase of CAPE (Fig 4) culminating in the largest values of CAPE observed towards the very end of the experiment. Significant amounts of upper level cloud associated with the convection was observed by the MMCR in this period (Blue line in Fig 5), but much less than during the monsoon (red curve). It is interesting to contrast the distribution of upper level clouds during the late monsoon period (January 26 – February 2) and the Break period (February 6 through the end of the experiment). The depth of cirrus layer was limited to altitudes above 10 km during the earlier period when the middle troposphere was very dry (Fig 3) but the cirrus layer was much deeper during the break period consistent with the moister conditions. It is evident from the typical example shown in Figure 6 that convection during this period was of a strongly continental character and was often related to mesoscale circulation features, such as the sea-breeze. The radar images (third column, Fig 6) exemplify the high intensity of the convection with reflectivities above 35 dBZ extending above 15 km on a regular basis. This

was accompanied by strong electrical activity, which was virtually absent in the earlier monsoon convection.

The convective regimes observed during TWP-ICE and described above constitute typical examples of continental, maritime and relatively shallow precipitating convection observed elsewhere in the tropics. This makes the TWP-ICE data set an ideal tool for the study of these convective types with an unprecedented level of detail. Opportunities for such studies will be highlighted in the next sections.

5. Observations that address key science goals

The range of weather sampled, the extensive continuous data collected from the surface sites and the large number of research flights, will allow us to address all the original science goals of the experiment. Of particular importance for the study of cirrus properties were the sampling of several anvils in both the monsoonal and break periods, and continental-like convection from clouds early in their lifecycle as well as a mature stage when the cirrus microphysical properties were dominated by new crystal growth. This will allow the study of the cirrus microphysics in relation to parent storm intensity and lifecycle. Preliminary indications are that the monsoon cirrus was characterised by both larger mean sizes and higher ice water contents than break period storms (A. Heymsfield, private communication). Other

flights included observations of the aging and vertical sorting of the cirrus as well as the sampling of highly aged cirrus being detrained from deep convection several hundred km to the south. There was also an emphasis on flying the high altitude aircraft over the ground-based remote sensing instruments at the Darwin ACRF site and on the Southern Surveyor. These flight legs included multiple spirals over the ACRF site and the resulting data will be an excellent resource for the validation of remotely sensed cloud properties.

Fresh anvil clouds in different regimes were observed on 2 and 6 February. For example, on the 6th February, break conditions were being established with easterly flow at 700 mb overlying westerlies at the surface. An isolated single-cell storm broke out over the north-east of the Tiwi Islands around 450 UTC, with radar echoes reaching 17 km. It produced a detached anvil which was advected north-westwards off the coast of the islands over the next two hours. The Proteus, Twin Otter, Dornier and Egrett (in that order) took off between 0535 and 0615 UTC. The Twin Otter remotely profiled the anvil along 11°15' and 11° 20' S while the Proteus spiralled down in the anvil from 47000' to 34000'. Meanwhile the Egrett transected the anvil at 40,000' and 42,000' along the same line as the Twin Otter, followed by a diagonal run at 44,000' (Fig. 7). At the lower level the Dornier flew around the storm at 1000' and 2500' after first making a detailed survey of its inflow (western) side. This day provides an excellent example of a single-cell island thunderstorm developing in low-aerosol conditions, in contrast with the more polluted higher aerosol example of 16 November (Vaughan et al 2006). Another example

was observations of a fresh anvil in the monsoon regime on 2 February. On this day, a convective cell associated with a system advancing from the northeast was observed to be developing over the Tiwi Islands just before takeoff. The anvil associated with this system dissipated rapidly given the dry ambient conditions on 2 February. The Proteus executed a series of spiral ascents and descents through this anvil, covering the entire life cycle of the system from a recently formed anvil to a dissipating anvil. Figure 8 shows selected CPI images as a function of altitude for the first spiral when the anvil was very young with the presence of plate-like, irregular, and aggregates of plate-like crystals. An automated shape analysis using various measures of crystal morphology showed that irregular particles dominated the population of particles with D > 100 μm irrespective of altitude. Similar to the case of the aged cirrus, particles with D < 100 μm were still dominantly quasi-spherical and made significant contributions to the total mass and extinction.

The observations in the fresh anvil can be contrasted with observations in aged cirrus obtained on other days during the project. For example, on 29 January 2006 the Proteus flew north-south and northeast-southwest oriented legs to measure the latitudinal dependence of the microphysical properties of cirrus bands generated by a low pressure system south of the TWP-ICE domain. Figure 9 shows ice crystals imaged by the SPEC CPI with maximum dimensions D greater than 100 μm. Pristine shapes, such as bullet rosettes or aggregates of bullet rosettes, appear regardless of altitude for these cirrus bands, all of which had minimum ages of approximately 4 hours which represents a strong contrast to plates and aggregates seen in Figure 8. The

automated habit classification scheme showed that bullet rosettes dominated the population of crystals with D > 100 μm with no statistically significant dependence on altitude. Crystals with D < 100 μm were predominantly quasi-spherical in shape and typically contributed more than half to the total mass and extinction and median mass diameters were usually between 50 and 100 μm. The observations in cirrus with various ages, combined with observations in the fresh anvils, present a unique opportunity to examine the relationship between ice microphysical properties and cirrus age, and in the case of anvil cirrus, with the intensity of the generating convection and proximity to the parent cell.

The data from all the microphysical probes in Table 4 are now being used to obtain the most accurate estimates of size and shape distributions of ice crystals and to estimate the bulk mass and single-scattering properties of the cirrus following techniques described by McFarquhar and Heymsfield (1996) and McFarquhar et al. (2002).. These data are being placed in the proper context through the use of the ground-based and airborne remote sensing data to better understand the myriad of factors that affect the cirrus microphysical properties and hence to determine how to better represent these properties in satellite and ground-based remote sensing algorithms. There were also many spiral ascents and descents performed over the ship and the ACRF site at Darwin providing valuable verification data for the remotely sensed microphysical retrievals of both ground based and space based observations such as CLOUDSAT and Calipso. One of these spiral

descents over the ACRF site was performed at the end of the 29 January cirrus mission. The cirrus layer as seen by the ACRF MMCR and MPL for the duration of the mission is shown in Figure 10. For much of the period, the lidar detects cirrus where the radar does not. This suggests low ice water content and small crystals in this layer.

The evolution of boundary-layer aerosol during the course of this experiment and its pre-monsoon partner provides an opportunity to study the effects of aerosol on deep convection. Similar meteorological conditions pertained at the beginning of November and mid-February, at the end of TWP-ICE: land-based afternoon convection triggered by sea breezes, exemplified by the afternoon storms on the Tiwi Islands. Detailed case studies of these storms were conducted during the two campaigns. The Dornier aerosol measurements showed a transition from copious biomass burning products (including black carbon) in mid-November, to cleaner conditions in December and extremely clean conditions in the inactive monsoon period when maritime air of Southern Hemisphere mid-latitude origin reached Darwin. Although aerosol amounts were higher in the subsequent break period, they were still a factor of 2-10 times less than in November, with negligible organic content compared to 1-2 μg m^{-3} in the earlier period. Interestingly, larger aerosols (> 1 μm) were around 5-10 times more prevalent in the two monsoon periods than in the pre-monsoon and break, consistent with the strong monsoonal westerlies. Modelling studies are currently under way to examine the impact of the different aerosol regimes on deep convection.

The comprehensive data set provides opportunities and challenges for the modelling community. The aim to provide high time-resolution forcing data sets to drive models was an integral part of the experiment design. Just as importantly the data collected by the aircraft and remote sensing systems (e.g., CPOL radar, profilers, ARM suite) provides an equally unique data set for the evaluation of these models, ranging from broad-scale characteristics of the convective systems to the details of microphysical parameterizations. The three meteorological and aerosol regimes that were sampled will provide an additional challenge – can the models represent these differences and how do they compare with observations? For example, it has been shown that models have particular difficulties representing convection reaching to the mid-troposphere only, as observed during the dry monsoon (Inness et al, 2001).

The radiosonde and surface flux measurements that will be used to force model simulations of the TWP-ICE period will also be very useful for process studies of the region. The array of radiosondes provides a detailed view of the diurnal cycle and evolution of the atmosphere at high temporal resolution while turbulent and radiative fluxes over a variety of surface types provide a detailed description of the surface energy balance. These measurements will be very useful for augmenting and interpreting long-term measurements available at Darwin from the Bureau and the ACRF site.

As well as the planned components, the weather that was sampled also provides a number of un-anticipated research opportunities. These include

the sampling of surface fluxes over warm tropical oceans at high wind speeds over several days. This data set has clear implications for the formation of intense tropical weather systems forced by surface fluxes such as tropical cyclones. Other systems that were sampled include a large MCS that developed distinct rotation within the experiment sampling domain. There is little doubt that this system would have spawned a tropical cyclone if it had remained over warm water instead of making landfall so again there are opportunities to look at the early stages of tropical cyclogenesis. The mature cyclone brought southern ocean mid-latitude air to Darwin, and survey flights of the Dornier and Egrett north-eastwards during this period measured the transition between this very clean air and air of Indonesian, and even Northern Hemisphereic origin with much higher concentrations of CO and particulates. Even data from the suppressed period near the middle of the campaign will be useful. During this period, clear sky radiative fluxes were obtained along with vertical profiles of temperature and humidity undisturbed by convection. These observations provide a very useful baseline for measurements obtained under other conditions.

6. Concluding Comments

The TWPICE experiment has succeeded in collecting an outstanding data set describing tropical cloud systems, their evolution and the interaction with the larger environment. It should be highlighted that the observations taken during TWPICE should be taken in the context of long-term observations of

clouds using remote-sensing techniques that are also available via the ARM web site (www.arm.gov). Data taken during the experiment include several tens of spiral ascents over the ground and airborne cloud radar/lidar combinations. These observations will serve as a valuable resource for both the development and validation of retrieval techniques as well placing the TWPICE observations in long term statistical contexts.

The TWPICE data set represents a major resource for the entire meteorological community. In terms of the range and completeness of the observations it represents one of the most comprehensive data sets of tropical cloud processes ever collected Much of the data is already available to the community through the ARM web site (http://www.archive.arm.gov/) as an IOP data set while UK supported aircraft data (Egrett and Dornier) will be made public in early 2008.

Acknowledgements.

TWPICE and ACTIVE were supported under the auspices of the US Department of Energy ARM Program, the ARM Uninhabited Aerospace Vehicle (UAV) Program, NASA Cloudsat, the UK Natural Environment Research Council (NERC) Grant Number NE/C512688/1, the NERC Airborne Remote Sensing Facility, the Australian National Marine Research Facility and the Bureau of Meteorology. Vaisala generously donated the radiosonde base stations. The Charles Darwin University, Darwin RAAF Base and the

Tiwi Island Land Council all made extensive facilities available to the experiment. More than 100 scientists were in the field. Particular thanks are due to retired Bureau of Meteorology Observers who led the operations of the remote sounding sites. Without the cooperation of a large team of specialists this experiment would not have been possible. We thank in particular the pilots, aircraft scientists and ground crew of the five aircraft for ensuring that the missions were so successful, and the staff of the Bureau of Meteorology Regional Centre in Darwin for their invaluable support both for forecasting and logistics. The whole experiment team is indebted to Brad Atkinson, Anthony Noonan, Tim Hume, Andrew Hollis and Lori Chappel whose untiring efforts made the experiment possible. Data were obtained from the ARM program archive, sponsored by DOE, Office of Science, Office of Biological and Environmental Research, Environmental Science Division.

References

Ackerman, T.P., and G. Stokes. 2003. "The Atmospheric Radiation Measurement Program." *Physics Today,* **56,** 38-45.

Beringer, J. and N. Tapper, 2002, "Surface energy exchanges and interactions with thunderstorms during the Maritime Continent Thunderstorm Experiment (MCTEX)." *J. Geophys. Res*, **107**, AAC 3-1 - AAC3-13.

Betz, H.-D., K. Schmidt, W. P. Oettinger, and M. Wirz, 2004: Lightning Detection with 3D-Discrimination of Intracloud and Cloud-to-Ground Discharges. *J. Geophys. Res. Lett.*, **31**, L11108, doi:10.1029/2004GL019821.

Clothiaux, E.E., T.P. Ackerman, G.G. Mace, K.P. Moran, R.T. Marchand, M.A. Miller, and B.E. Martner, 2000: Objective determination of cloud heights and radar reflectivities using a combination of active remote sensors at the ARM CART sites. *J. Appl. Met., 39*, 645-665.

Drosdowsky, W., 1996: Variability of the Australian summer monsoon at Darwin: 1957-1992, *J. Clim.*, **9**, 85-96.

Ecklund, W.L. C R. Williams, P.E. Johnston and K.S. Gage. 1999: A 3-GHz Profiler for Precipitating Cloud Studies, *J. Atmos. Oceanic Tech.,* **16**, 309–322

Fairall, C. W. E. F. Bradley, J. E. Hare, A. A. Grachev and J. B. Edson. 2003: Bulk Parameterization of Air–Sea Fluxes: Updates and Verification for the COARE Algorithm**,** *J. Clim.,* **16**, 571–591.

Garrett, T.J., B.C. Navarro, C.H. Twohy, E.J. Jensen, D.G. Baumgardner, P.T. Bui, H. Gerber, R.L. Herman, A.J. Heymsfield, P. Lawson, P. Minnis, L. Nguyen, M. Poellot, S.K. Pope, F.P.J. Valero, and E.M. Weinstock, 2005. Evolution of a Florida cirrus anvil. J. Atm. Sci., 62, 2352-2372.

Godfrey, J.S., E.F. Bradley, P.A. Coppin, L.F. Pender, T.J. McDougall, E.W. Schulz, and I. Helmond, 1999: Measurements of upper ocean heat and freshwater budgets near a drifting buoy in the equatorial Indian Ocean. *J. Geophys. Res.*, **104**, C6, 13,269-13,302.

Hamilton ,K., R.A. Vincent and P.T. May, 2004: The DAWEX field campaign to study gravity wave generation and propagation, *J. Geophys. Res*., **109**, D20S01, doi:10.1029/2003/JD004393.

Heymsfield, A.J., and G.M McFarquhar, 1996. High albedos of cirrus in the tropical Pacific Warm pool: microphysical interpretations from CEPEX and from Kwajalein, Marshall Islands. J. Atm. Sci., 53, 2424-2451.

Heymsfield, A.J., Z. Wang, and S. Matrosov, 2005. Improved radar ice water content retrieval algorithms using coincident microphysical and radar measurements. J. App. Met., 44, 1391-1412.

Hogan, R.J., A.J. Illingworth and H. Sauvageot, 2000:, Measuring Crystal Size in Cirrus Using 35- and 94-GHz Radars, *J. Atmos. Oceanic Tech*., **17**, 27-37.

Inness, P.M., J.M. Slingo, S.J. Woolnough, R.B. Neale, and V.D. Pope, 2001: Organization of tropical convection in a GCM with varying vertical resolution: Implications for the simulation of the Madden-Julian Oscillation. Clim. Dyn, **17**, 777-793.

Keenan, T.D., 2003: Hydrometeor classification with a C-band polarimetric radar, *Aust. Meteor. Mag.*, **52**, 23-31

Keenan, T.D. and R.E. Carbone, 1992: A preliminary morphology of precipitation systems in tropical northern Australia, *Quart. J. Roy. Meteor. Soc*., **118**, 283-326.

Keenan, T.D. and Manton, M.J,. 1996: Darwin climate monitoring and research station: observing precipitating systems in a monsoon environment. BMRC Research Report No. 53, Bur. Met. Australia.

Keenan, T.D., J. McBride, G. Holland, N. Davidson, and B. Gunn, 1989: Diurnal variations during the Australian Monsoon Experiment (AMEX) Phase II. *Mon. Wea. Rev.,* 117, 2535–2553.

Keenan, T., K. Glasson, F. Cummings, T.S. Bird, J. Keeler, and J. Lutz, 1998: The BMRC/NCAR C-Band Polarimetric (C-Pol) Radar System. *J. Atmos. Oceanic Tech.*, **15**, 871-886.

Keenan, T., S. Rutledge, R. Carbone, J. Wilson, T. Takahashi, P. May, N. Tapper, M. Platt, J. Hacker, S. Sekelsky, M. Moncrieff, K. Saito, G. Holland, A. Crook and K. Gage, 2000: The Maritime Continent Thunderstorm Experiment (MCTEX): Overview and some results, *Bull. Amer. Meteor. Soc*., **81**, 2433-2455.

Mapes, B. and R.A. Houze Jr., 1992: An integrated view of the 1987 Australian monsoon and its mesoscale convective systems Part 1: Horizontal structure, *Quart. J. Roy. Meteor. Soc*., **118**, 927-963.

Mather, J.H., T.P. Ackerman, W.E. Clements, F.J. Barnes, M.D. Ivey, L.D.Hatfield, and R.M. Reynolds. 1998. "An Atmospheric Radiation and Cloud Station in the Tropical Western Pacific." *Bull. Amer. Meteor. Soc.,* **79**, 627–642.

Mather, J.H., S.A. McFarlane, M.A. Miller, and K.L. Johnson, 2006. Cloud Properties and associated heating rates in the Tropical Western Pacific. *J. Geophys. Res*., Accepted.

May, P.T. and A. Ballinger, 2007: The statistical characteristics of convective cells in a monsoon regime (Darwin, Northern Australia), *Mon. Wea. Rev*., **135**, 82–92.

May,P.T. and T.D. Keenan, 2005: Evaluation of microphysical retrievals from polarimetric radar with wind profiler data, *J. Appl. Meteor.* **44**, 827–838.

McFarquhar, G.M. and A.J. Heymsfield. 1996: Microphysical Characteristics of Three Anvils Sampled during the Central Equatorial Pacific Experiment. *J. Atmos. Sci.,* **53**, 2401–2423.

McFarquhar, G.M., P. Yang, A. Macke, and A.J. Baran, 2002: A new parameterization of single-scattering solar radiative properties for tropical ice clouds using observed ice crystal size and shape distributions. *J. Atmos. Sci.*, **59**, 2458-2478.

Russell, P.B., L. Phister and H.B. Selkirk, 1993: The Tropical Experiment of the Stratosphere-Troposphere Exchange Project (STEP): science objectives, operations, and summary findings, *J. Geophys. Res*., **98**, 8563-8589.

Westwater, E.R., S. Crewell, and C. Mätzler, 2005. Surface-based microwave and millimeter wave radiometric remote sensing of the troposphere: a tutorial. *IEEE Geosci. Rem. Sens. News.*, http://www.grss-ieee.org, March, 16-33.

Whiteway, J., C. Cook, M. Gallagher, T. Choularton, J. Harries, P. Connolly, R. Busen, K. Bower, M. Flynn, P. T. May, R. Aspey and J. Hacker, 2004: Anatomy of cirrus clouds: Results from the Emerald airborne campaigns, *Geophys. Res. Lett*., **31**, L24102, doi:10.1029/2004GL021201

Vaughan, G.V., C. Schiller, R. MacKenzie, K. Bower, T. Peter, H. Schlager, N. R. P Harris and P. T. May, 2006, Studies in a natural laboratory: High-altitude aircraft measurements around deep tropical convection, *Bull. Amer. Meteor.Soc*, submitted companion paper

Vincent, R.A., S. Dullaway, A. MacKinnon, I.M. Reid, F. Zinc, P.T. May and B. Johnson, 1998: A VHF boundary layer radar: First results, Radio Sci., **33**, 845-860.

Webster, P.J., and R. Lukas, 1992, TOGA COARE: The Coupled Ocean—Atmosphere Response Experiment*, Bull. Amer. Meteor. Soc*., *73*, 1377-1416.

Zhang, M.H., Lin, J.L., Cederwall, R.T., Yio, J.J. and Xie, S.C., 2001: Objective analysis of ARM IOP data: Method and sensitivity. *Mon. Wea. Rev.*, **129**, 295-311.

Table Captions

Table 1. Science goals for TWPICE and ACTIVE

Table 2. Permanent instruments in the Darwin area associated with the Australia Bureau of Meteorology and the DOE ARM Climate Research Facility.

Table 3. Instruments deployed in the Darwin area for TWP-ICE.

Table 4. Aircraft Instruments and observational capabilities. Detailed tables including the aircraft instruments are available on line

Table5. TWP-ICE Aircraft Missions.

Figure captions

Figure 1. The TWP-ICE/ACTIVE experiment domain. The large blue circle indicates a 150 km radius centred on the C-Pol radar. The small circle near 130E indicates the operating region of the Southern Surveyor. The two interlocking circles near the center of the domain indicate the dual-Doppler lobes associated with the C-Pol and Berrima radars. Additional ground-based instruments are listed in Tables 2 and 3.

Figure 2 Area averaged rainfall accumulation estimated using the polarimetric radar. The period from January 13 up to January 22 was an active monsoon, with a major MCS developing on January 23. The following period was a suppressed monsoon with relatively shallow storms. The transition to the break on February 6 was preceded by three completely clear days.

Figure 3 Time height cross-section of relative humidity from Point Stuart radiosondes. Relative humidity is given with respect to liquid water at all altitudes.

Figure 4 Time series of area mean CAPE (red curve) and the area averaged hourly rain rate (black curve). The CAPE is calculated from the 5 sounding sites using un-modified soundings and taking the parcel from 100 m.

Figure 5 Cloud frequency profiles for the four regimes and the dry days The period January 21-25 was active monsoon, January 26 to February 2 was a suppressed monsoon period, February 3-5 were clear and February 6 to 13 were active break periods (see text for details).

Figure 6 Sample IR satellite images from MTSAT1-R of top end, radar PPI maps and typical radar cross-sections for the three rain regimes. These were active monsoon (left panels), suppressed monsoon (middle panels) and break period (right panels). Note that these panels are not necessarily at the same dates and times, but were rather chosen as representative of typical structure and organisation observed in these periods. The IR enhancement is T > 250 K is gray scale, 250 – 230 K are blue shades, 230 - 210 K are green shades, 210 - 190 K are yellow shades and T < 190 are red shades. Radar contours are drawn every 10 dBZ from 10 dBZ

Figure 7 Rain map from the polarimetric radar at 0710 UT on February 6, 2006. Contours are drawn every 20 mm/hr from 0 mm/hr. Aircraft tracks from the Twin Otter (green) , Egrett (red) and Proteus (blue) are overlaid. The circles mark the aircraft position and tracks are drawn for +/- 1 hour around the radar scan time (0710 UTC) for the Twin Otter and Egrett and +/- 10 minutes for the Proteus.

Figure 8 SPEC Cloud Particle Imager (CPI) images of ice crystals with D > 100 μm in a fresh monsoonal thunderstorm anvil from February 2, 2006 showing a mixture of quasi-spherical and chain crystal habits.

Figure 9 CPI images of ice crystals with D > 100 μm in an aged anvil on January 29 showing large numbers of bullet rosettes.

Figure 10. Time series of lidar backscatter (top panel) and radar reflectivity (bottom panel) observed from the Darwin ACRF site on January 29, 2006 . The thin cirrus layer near 12 km is associated with outflow from the large low pressure region several hundred kilometres to the south of Darwin.

Table 1. Science goals for TWPICE and ACTIVE

1) Collect detailed measurements of the cirrus microphysics and relate them to storm intensity and proximity (spatial and temporal) to the parent convection.
2) Relate measurements of aerosol and chemical species in the outflow of deep convection, and in the surrounding TTL, to low-level sources and identify how the deep convection has modified the aerosol population in the anvils.
3) Compare the concentration of aerosol and chemical tracers (with a range of lifetimes and origins) in the outflow with that in the background TTL, and therefore determine the contribution of convection to the composition of the TTL including NOx and O_3 over Darwin
4) Improve and evaluate cloud property retrievals from satellite-based and the ground-based remote sensing measurements.
5) Provide data sets for forcing and evaluating cloud resolving and single column models that will attempt to simulate the observed cloud system characteristics.
6) Document the evolution of oceanic convective clouds from the early convection phase through to the remnant cirrus with particular emphasis on their microphysics.
7) Measure the dynamical and radiative impacts of the cloud systems.
8) Characterize the environment in which the cloud systems occur.
9) Document the evolution of the convective boundary layer throughout the diurnal cycle and through the lifecycle of convective systems.
10) Observe the characteristics of convectively generated gravity waves.

Table 2. Permanent instruments in the Darwin area associated with the Australia Bureau of Meteorology and the DOE ARM Climate Research Facility.

Instrument/System	Description
Bureau of Meteorology	
5.6 GHz Scanning Polarimetric Radar	Provides 3-dimensional hydrometeor distributions with a range of approximately 150 km, located 20 km NE of Darwin
Operational Scanning Doppler weather radar	Provides spatial distribution of convection/precipitation. Located approximately 10 km SE of Darwin.
50 MHz Wind Profiler	Vertical profiles of wind, located 10 km SE of Darwin
920 MHz Wind Profiler	Vertical profiles of wind and precipitation, located 10 km SE of Darwin
Automated Weather Stations	Pressure, temperature, humidity, and wind speed and direction at 10 sites around the Northern Territory
Rain Gauge Network	
DOE ARM Climate Research Facility	
Millimeter Cloud Radar	35 GHz Doppler radar, provides cloud boundaries and used to derive microphysical properties
Micropulse Lidar	532 nm lidar, provides cloud boundaries and used to derive cloud optical properties
Vaisala Ceilometer	Provides cloud base to a maximum altitude of 7 km and profiles of backscatter at 1
Total Sky Imager	Hemispheric digital camera provides digital snapshots of the sky and pixel by pixel cloud cover determination
Atmospheric Emitted Radiance Interferometer	Measures infrared emission from atmosphere in range 520-3300 cm^{-1} with 1 cm^{-1} resolution
Microwave Radiometer	23.8/31.4 GHz, provides total column water vapor and liquid water
Multi-Filter Rotating Shadow-band Radiometer	Six narrowband channels between 0.4 and 1 mm provide column aerosol information
Disdrometer	Rain drop size distribution
Broadband Radiometers	Up and down-looking Eppley solar and terrestrial infrared radiometers
Surface Meteorology	Pressure, Temperature, Humidity, Rain Rate, Wind speed and direction

Table 3. Instruments deployed in the Darwin area for TWP-ICE.

Instrument/ System	Location	Description	PI/Affiliation
Radiosonde Array	Perimeter of TWP-ICE Domain	Profiles of temperature, humidity, and wind	ACRF/Bureau / Vaisala
Flux Network	Four sites over water, marsh and savannah (2)	Eddy correlation latent and sensible heat fluxes and surface radiation	Tapper (Monash U.)
50 MHz Profiler	Darwin ACRF site	Vertical profiles of wind	Vincent (U. Adelaide)
3 GHz Profiler	Bureau profiler site	Vertical profiles of precipitation	Williams (NOAA)
Radiometer Network	Garden Point and Cape Don	Down-welling broadband solar and terrestrial infrared fluxes	Long (PNNL)
LINET Lightning Network	Perimeter of TWP-ICE Domain	Multi-antenna lightning detection operating in the VLF/LF range	Hoeller (DLR)
Lightning Sensor	Darwin ACRF Site	VHF Broadband Digital Interferometer for high temporal resolution lightning monitoring	Kawasaki (Osaka U.)
HATPRO	Darwin ACRF Site	14 Channel microwave radiometer: profiles of temperature and water	Crewell (U. Munich)
Radiative Fluxes	Southern Surveyor	Broadband solar and terrestrial infrared fluxes and SST	Reynolds (BNL)
Bulk Fluxes	Southern Surveyor	Sensible and latent heat fluxes	Bradley (CSIRO)
PARSL	Southern Surveyor	Cloud radar, cloud lidar, ceilometer, microwave radiometer, temperature, humidity, and precipitation	Mather (PNNL)
M-AERI	Southern Surveyor	Marine Atmospheric Emitted Radiance Interferometer,	Minnett (U. Miami)
Oceanographic Observations	Southern Surveyor	Salinity, temperature, and current profiles	Tomczak (Flinders University)

Table 4. Aircraft Instruments and observational capabilities. Detailed tables including the aircraft instruments are available on line

Aircraft	Altitude range	Observation type
ARA Dimona	10m -2km	State parameters, Turbulence, SW and LW radiation
NERC Dornier	100m- 4 km	State parameters Aerosol size distribution Aerosol composition Ozone, CO, Hydrocarbons and Halocarbons
Twin Otter	1 km -3 km	NASA 96 GHz cloud radar York University 530 nm polarisation lidar
ARA Egrett	8-15 km	State parameters Upper tropospheric humidity Cloud particle size distributions Ice Cloud particle habit Aerosol size distribution Black carbon aerosol Ozone, CO, NO_x Hydrocarbons and halocarbons
ARM-UAV Proteus	8-16 km	State parameters Cloud particle size distributions 10 μm to ~ 1.5 mm Cloud particle habit 10 μm to ~ 1 mm Total water content and extinction Cloud aerosol 0.35 to 50 μm SW and LW radiation 1.053 μm lidar CO and CO_2 sensors

Table5. TWP-ICE Aircraft Missions.

Date	Cloud Missions		Survey Missions		Other Missions	
	Aircraft	Mission	Aircraft	Mission	Aircraft	Mission
20 Jan	E N	MA				
21 Jan			D	L		
22 Jan	E N T	MA				
23 Jan	E T	MA				
25 Jan	E P T	AC	D N	L M		
26 Jan			N	L		
27 Jan	E P T	AC	N	L		
29 Jan	P T	AC	D	L		
30 Jan			N	M		
31 Jan			D	L	E	Li
1 Feb			D N	L L	E	Li
2 Feb	D P T	MA	N	L		
3 Feb			E N	M M	T	TO
4 Feb			D	M	P	CO
5 Feb			D	M		
6 Feb	E P T	BA	D	M		
8 Feb	D E N T	BA				
9 Feb	E	BA				
10 Feb	D E N P T	BA	D	M		
12 Feb	D E N P T	BA				
13 Feb	E	BA	D	L		
14 Feb					E N	I I

Aircraft: D = Dimona, E=Egrett, N = Dornier, P=Proteus, T=Twin Otter

Cloud Missions: MA=Monsoon Anvil, AC=Aged Cirrus, BA=Break Anvil

Survey Missions: L=Land Survey, M = Maritime Survey

Other Missions: TO=Terra Overpass, CO = Clear sky CO profile, I=Intercomparison, Li = Lidar

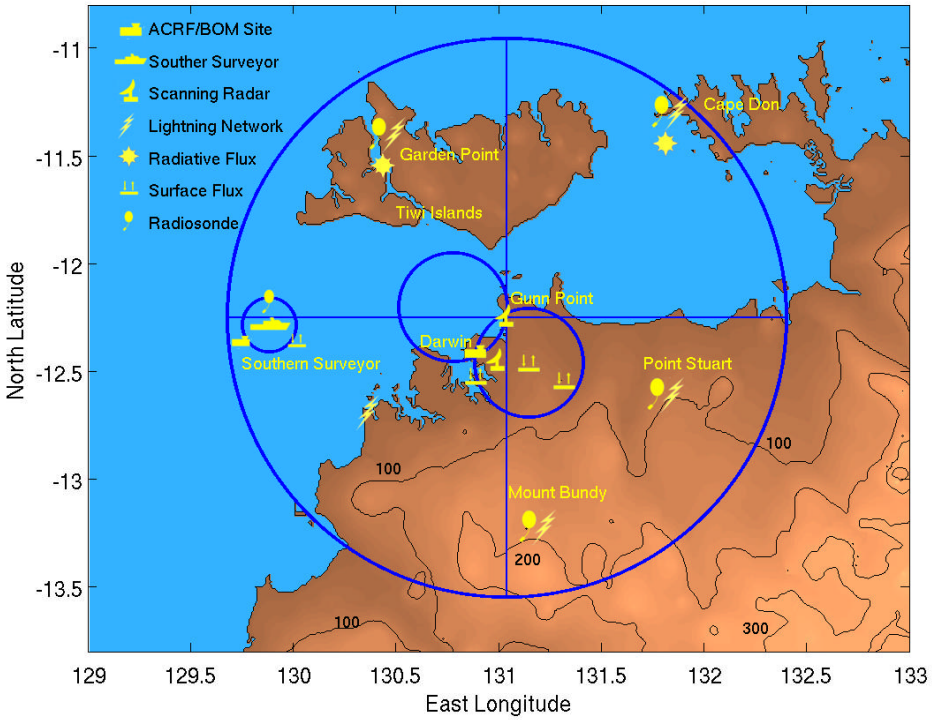

Figure 1. The TWP-ICE/ACTIVE experiment domain. The large blue circle indicates a 150 km radius centered on the C-Pol radar. The small circle near 130E indicates the operating region of the Southern Surveyor. The two interlocking circles near the center of the domain indicate the dual-Doppler lobes associated with the C-Pol and Berrima radars. Additional ground-based instruments are listed in Tables 2 and 3.

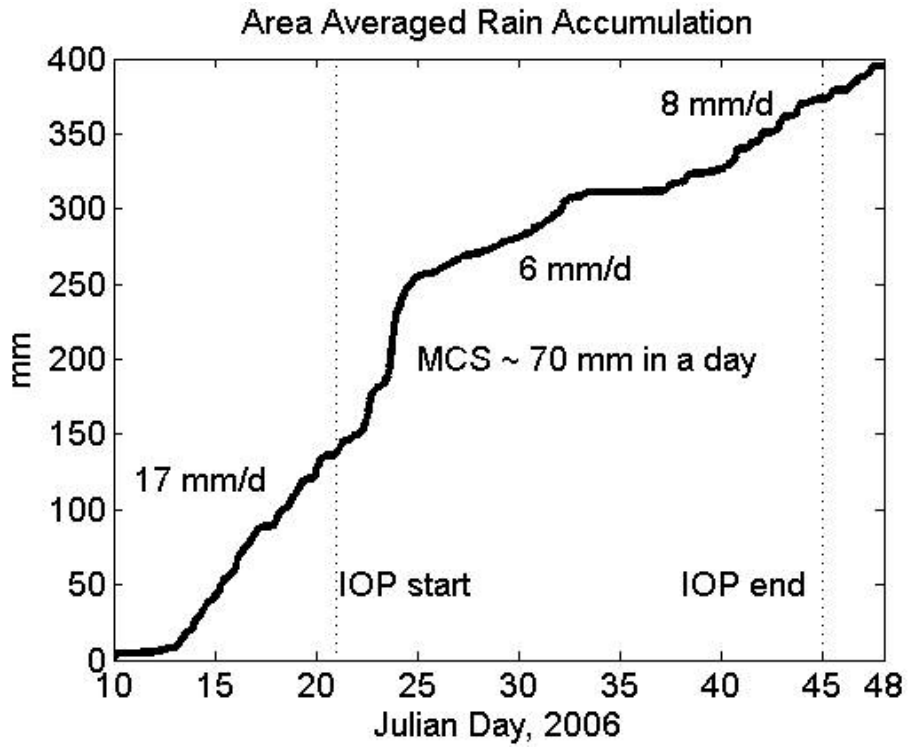

Figure 2 Area averaged rainfall accumulation estimated using the polarimetric radar. The period from January 13 up to January 22 was an active monsoon, with a major MCS developing on January 23. The following period was a suppressed monsoon with relatively shallow storms. The transition to the break on February 6 was preceded by three completely clear days.

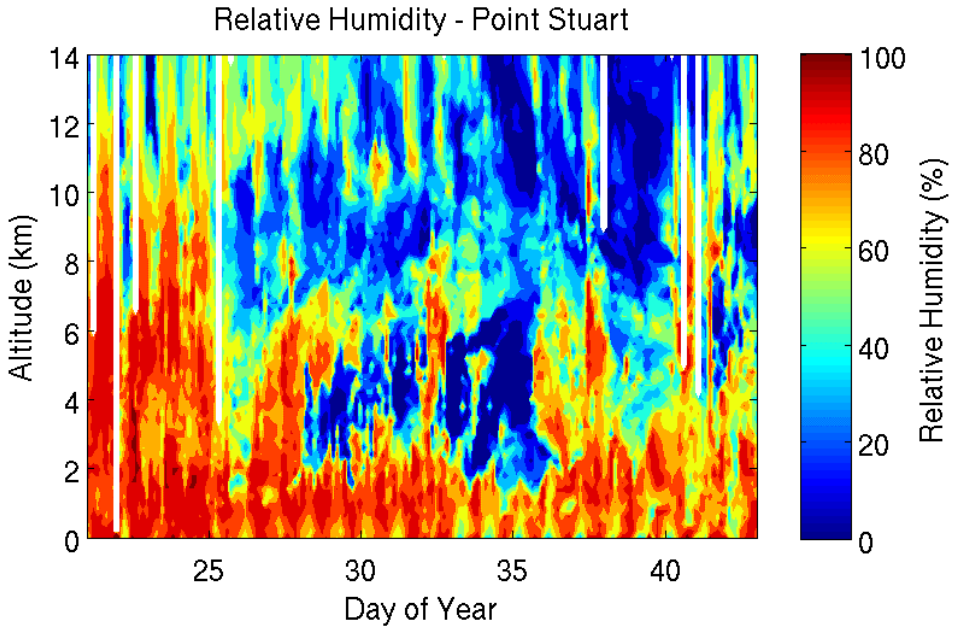

Figure 3 Time height cross-section of relative humidity from Point Stuart radiosondes. Relative humidity is given with respect to liquid water at all altitudes.

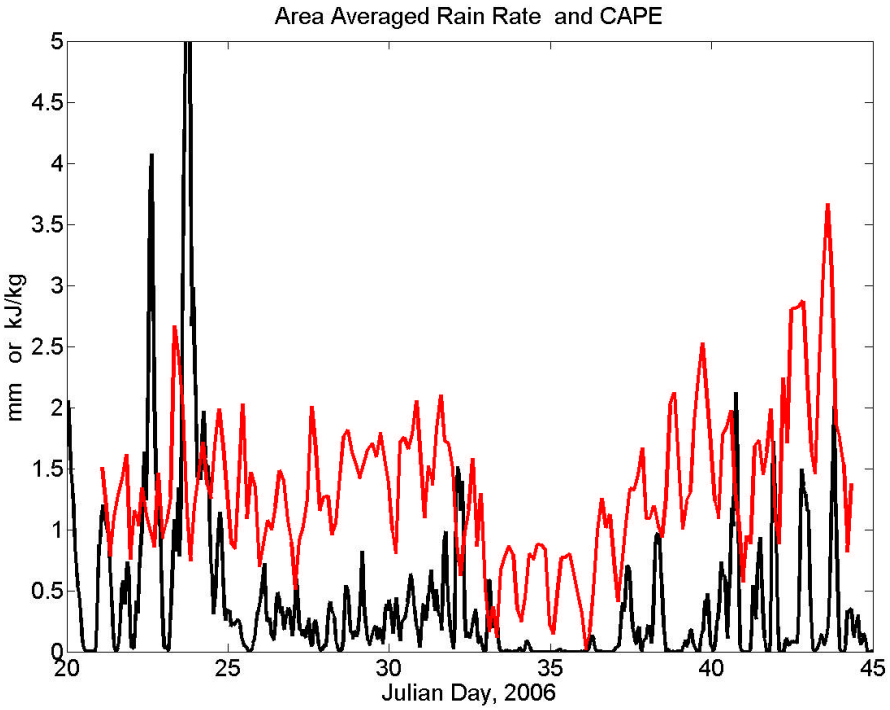

Figure 4 Time series of area mean CAPE (red curve) and the area averaged hourly rain rate (black curve). The CAPE is calculated from the 5 sounding sites using un-modified soundings and taking the parcel from 100 m.

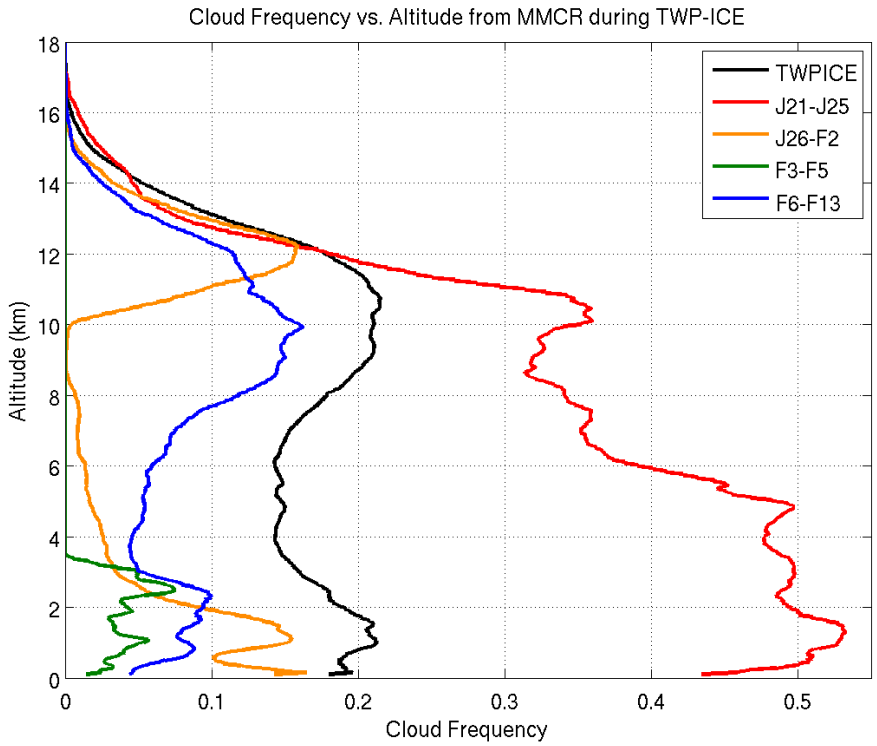

Figure 5 Cloud frequency profiles for the four regimes and the dry days The period January 21-25 was active monsoon, January 26 to February 2 was a suppressed monsoon period, February 3-5 were clear and February 6 to 13 were active break periods (see text for details).

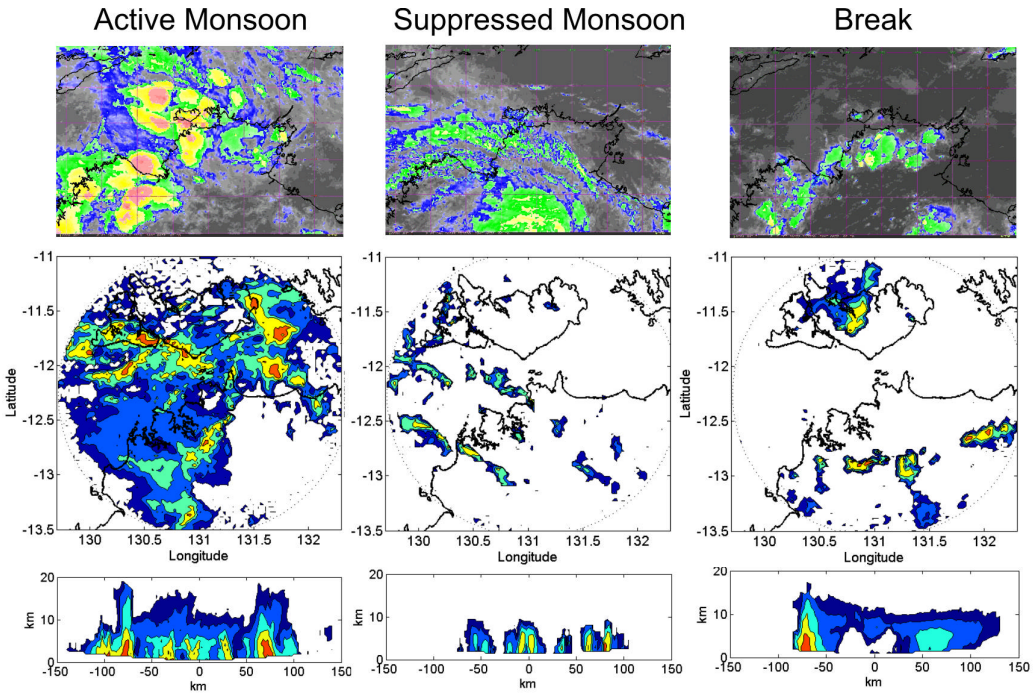

Figure 6 Sample IR satellite images from MTSAT1-R of top end, radar PPI maps and typical radar cross-sections for the three rain regimes. These were active monsoon (left panels), suppressed monsoon (middle panels) and break period (right panels). Note that these panels are not necessarily at the same dates and times, but were rather chosen as representative of typical structure and organisation observed in these periods. The IR enhancement is T > 250 K is gray scale, 250 – 230 K are blue shades, 230 - 210 K are green shades, 210 - 190 K are yellow shades and T < 190 are red shades. Radar contours are drawn every 10 dBZ from 10 dBZ

.

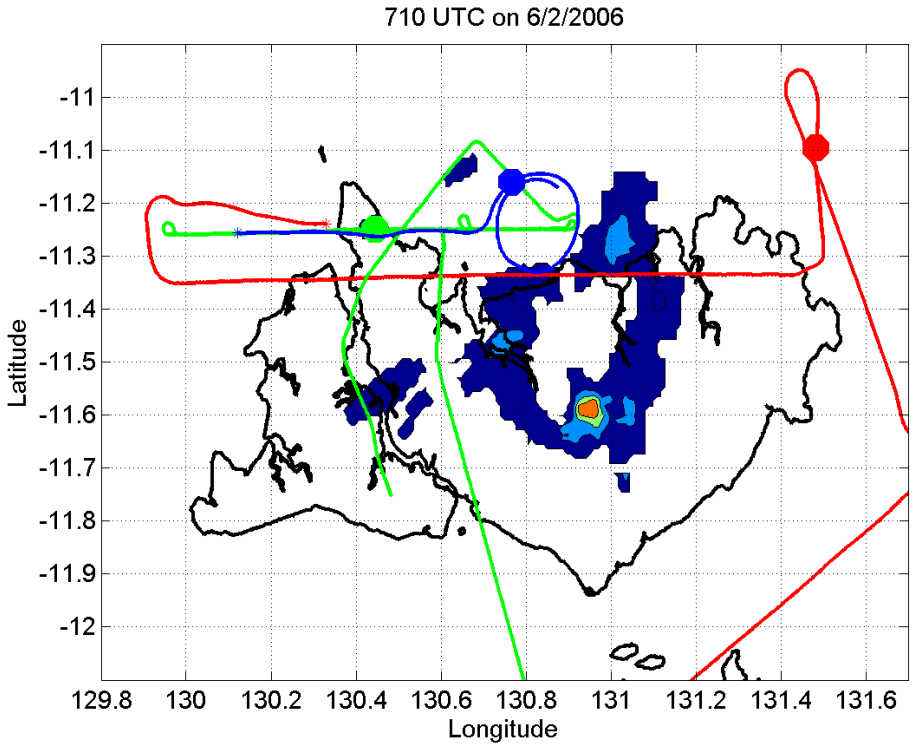

Figure 7 Rain map from the polarimetric radar at 0710 UT on February 6, 2006. Contours are drawn every 20 mm/hr from 0 mm/hr. Aircraft tracks from the Twin Otter (green) , Egrett (red) and Proteus (blue) are overlaid. The circles mark the aircraft position and tracks are drawn for +/- 1 hour around the radar scan time (0710 UTC) for the Twin Otter and Egrett and +/- 10 minutes for the Proteus.

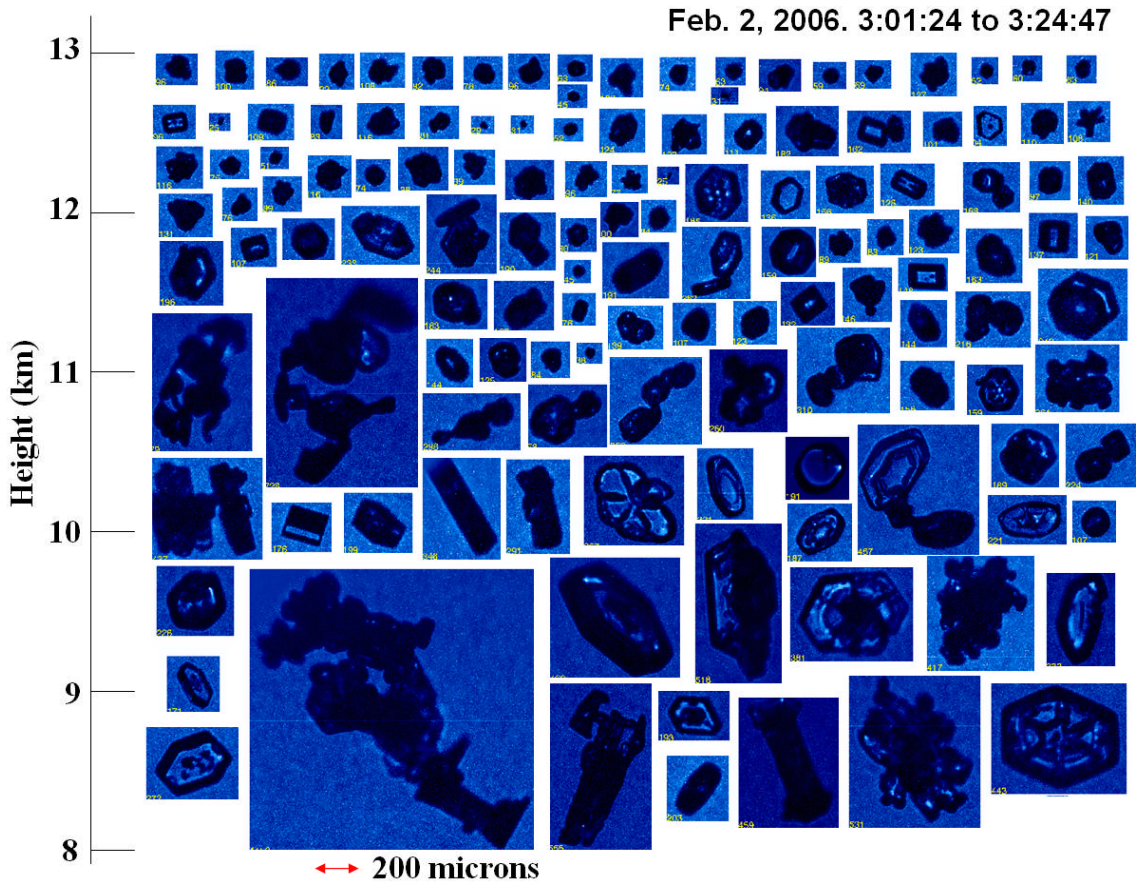

Figure 8 SPEC Cloud Particle Imager (CPI) images of ice crystals with D > 100 μm in a fresh monsoonal thunderstorm anvil from February 2, 2006 showing a mixture of quasi-spherical and chain crystal habits.

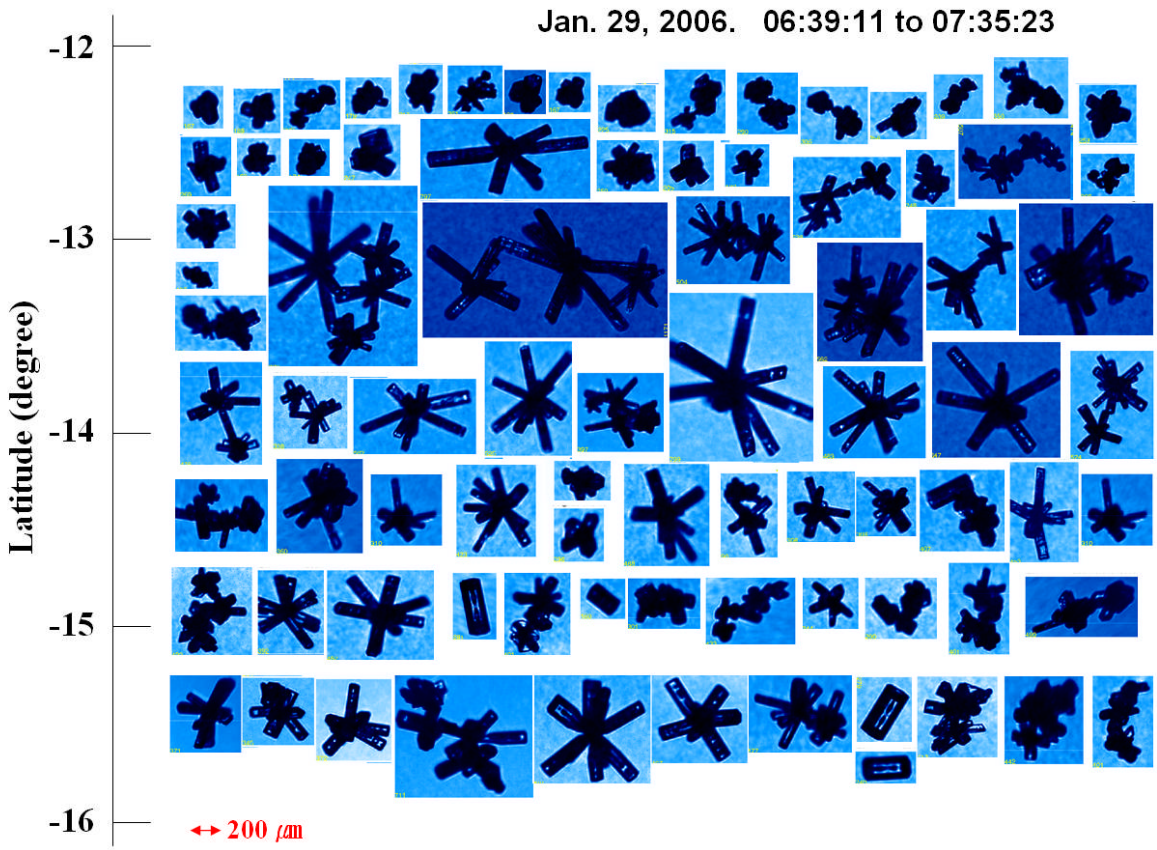

Figure 9 CPI images of ice crystals with D > 100 μm in an aged anvil on January 29 showing large numbers of bullet rosettes.

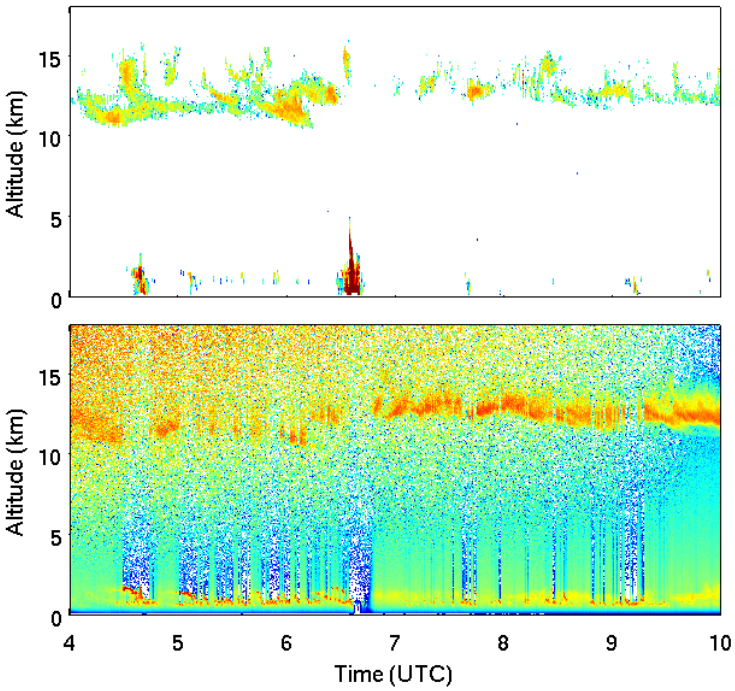

Figure 10. Time series of lidar backscatter (top panel) and radar reflectivity (bottom panel) observed from the Darwin ACRF site on January 29, 2006 . The thin cirrus layer near 12 km is associated with outflow from the large low pressure region several hundred kilometres to the south of Darwin.

On line tables

On-line Table 1: In-situ and remote sensing instruments in the ARM UAV suite of instruments installed on the Proteus

Instrument	Operating Range	Derived Parameters	Description
Cloud Particle Imager (CPI)	10 μm to ~ 1 mm	2.3 μm resolution images, SDs	Images recorded on CCD array
Cloud Aerosol Spectrometer (CAS)	0.35 to 50 μm	SDs	Detects forward scattered light from small particles
Cloud Droplet Probe (CDP)	2 to 50 μm	SDs	Open path probe detecting forward scattered light from small particles
Cloud Imaging Probe (CIP)	50 μm to 1.6 mm	SDs; two-dimensional images	Shadowing of photodiodes
Counterflow virtual impactor (CVI)	Particles > 5 μm included in bulk estimates	Bulk measure of IWC	Evaporator probe
Nevzorov Probe	Bulk measurement	LWC, TWC	Hot wire probe
Cloud Integrating Nephelometer (CIN)	Bulk measurement	βe, asymmetry parameter	Detects directional scattering of scattered light
Sandia Dual Path Laser Hygrometer (TDL)	Vapor measurements to 1 ppmv at 50 Hz	Water vapor	Near-infrared laser absorption spectroscopy at short (13.4 cm) and long (403 cm) paths
Cryogenic Hygrometer (CR2)	Measures T_f to -105°C, response time of 10 to 20 s	Water vapor	Closed cycle cryogenically cooled mirror
High-altitude fast response in-situ CO_2 analyzer	±0.1 ppmv	CO_2 mixing ratio	Absorption at 4.6 μm measured relative to reference gas of known concentration
MicroMaps CO instrument		CO mixing ratio and total column tropospheric CO	Multi-channel gas filter radiometer
Infrared Thermometers (IRTs)	Two, operating from 8 to 10 μm and 9.6 to 11.5 μm	Brightness temperature	Two 2.5° field of view downwelling infrared thermometers
Pyrgeometers	4 to 40 μm	Radiance	CG4 model: zenith on level platform; nadir pod; nadir gold covered
Pyranometers	0.4 to 4.0 μm	Radiance	Five Kipp and Zonen CM-22s: zenith on level platform; zenith fixed; nadir pod; nadir pod (single

			inner dome); pod (silver covered)
Spectral Radiance Package (SRP)	Three, from 385 to 1050, 720 to 800, &1300 to 1500 nm	Upwelling spectral radiance	Narrow field of view
Diffuse Field Camera (DFC)	Two, centered at 645 and 1610 nm	Directional dependence of radiance	Imaging cameras measuring hemispheric upwelling radiance
MicroAir Data Transducer (MADT)		Pressure, Pressure altitude, Temperature, Mach number, True air speed	Measurements of payload and atmospheric state parameters

On-line Table 2: Instrumentation on the Egrett

Instrument	Measurement	PI
Basic Meteorology and position	Pressure, temperature, wind, GPS (1 Hz)	Jorg Hacker, Airborne Research Australia
DMT Single Particle Soot Photometer (SP-2) †	Aerosol particle size distribution (0.2 – 1.0 μm), light-absorbing fraction and composition	Hugh Coe, Univ. Manchester, UK
2 x TSI-3010 Condensation Particle Counter (CPC)	Total condensation particles > 10 nm & > 80 nm	Martin Gallagher, Univ. Manchester, UK
DMT Cloud, Aerosol & Precipitation Spectrometer (CAPS)	Cloud droplet spectrum, aerosol/small particle asymmetry, aerosol refractive index, (diameter 0.3- 2000 μm)	Andy Heymsfield, NCAR, Boulder, USA
DMT Cloud Droplet Probe (CDP)	Cloud Particle Size Distribution (diameter 2 - 62 μm)	Martin Gallagher, Univ. Manchester, UK
SPEC Cloud Particle Imager CPI-230	Cloud particle/ice CCD images, (diameter 10 - 2,300 μm)	Martin Gallagher, Univ. Manchester, UK
Buck Research CR-2 frost point hygrometer	Ice point temperature, 20 s, ± 0.1°	Reinhold Busen, DLR, Germany
Open path tuneable diode laser hygrometer	Water vapour concentration, 1s, ±1 ppmv	Jim Whiteway, York Univ., Canada
Closed path tuneable diode laser hygrometer	Water vapour concentration, 1s, ±1 ppmv	Geraint Vaughan, Univ. Manchester, UK
CO analyser	Carbon monoxide, 1 Hz, ± 2 ppbv	Andreas Volz-Thomas, FZ Jülich, Germany
Miniature Gas-Chromatograph	Halocarbons (Cl, Br, I), 3-6 min, ± 5%	Neil Harris, Univ. Cambridge, UK
TE-49C UV Ozone sensor	Ozone concentration (± 2 ppbv, 10 seconds)	Reinhold Busen, DLR, Germany
Automatic Tube Sampler (ATS), 15 samples per flight	C4-C9, Non-methane hydrocarbons, monoterpenes and OVOCs	Alastair Lewis, Univ. York, UK
NO and NO_2 chemiluminescent detector †	± 200 ppt @ 10 Hz; ± 30 ppt @ 4 s integration	Andreas Volz-Thomas, FZ Jülich, Germany

† alternates (only one flown at any time)

Online Table 3 Twin Otter payload

Instrument	Measurement	PI/ Institute
95 GHz cloud radar	Radar reflectivity (minimum ~-35 dBZ)	S. Dinardo, Jet Propulsion Laboratory, NASA
532 nm lidar	Backscatter power, depolarisation ratio	J. Whiteway, York University

Online Table 4: Dornier payload

:

Instrument	Measurement	PI
Aventech AIMMS-20 probe	GPS position, pressure, temperature, relative humidity, winds, 1 Hz	David Davies, ARSF
Aerodyne Aerosol Mass Spectrometer	Aerosol size and composition, 30 – 2000† nm	Hugh Coe, Univ. Manchester, UK
TSI3010 Condensation particle counter	Aerosol concentration > 10 nm, 1 Hz	Martin Gallagher, Univ. Manchester, UK
Grimm Optical Particle Counter Model 1.108	Aerosol size distribution, 0.3 – 2† µm, bins 0.1 – 0.2 µm, 0.16 Hz	Martin Gallagher, Univ. Manchester, UK
Ultra high sensitivity aerosol spectrometer	Aerosol size distribution 0.3 – 0.8 µm, 7.5 nm bins, 1 Hz.	Martin Gallagher, Univ. Manchester, UK
DMT Aerosol spectrometer probe ASP-100	Aerosol size distribution, 0.2 – 2† µm, bins 0.03 – 0.5 µm, 0.1 Hz	Martin Gallagher, Univ. Manchester, UK
Forward scattering spectrometer probe (FSSP)	Aerosol and cloud droplet size distribution, 0.5 - 32 µm, bin 0.8 µm, 0.1 Hz	Martin Gallagher, Univ. Manchester, UK
Particle soot absorption spectrometer (PSAP)	Black carbon concentration (aerosol), ± 1 µg m^{-3}, 0.2 Hz	Andreas Minnikin, DLR, Germany
Filters	Coarse aerosol composition, whole flight accumulation	Keith Bower, Univ. Manchester, UK
2B technologies model 202 ozone monitor	Ozone concentration, ±2 ppbv, 0.1 Hz	Alastair Lewis, Univ. York, UK
Aerolaser AL5003	Carbon monoxide concentration, ± 1 ppbv, 1 Hz	Alastair Lewis, Univ. York, UK
Automatic Tube Sampler (ATS), 15 samples per flight	C4-C9, Non-methane hydrocarbons, monoterpenes and OVOCs	Alastair Lewis, Univ. York, UK
Chemiluminescence/catalysis	$NO/NO_x/NO_y$	James Lee, Univ. York, UK
Miniature Gas-Chromatograph	Halocarbons (Cl, Br, I), 3-6 min, ± 5%	Neil Harris, Univ. Cambridge, UK

† Upper bound limited by inlet efficiency

Online Table 5: ECO-Dimona instrumentation

Instrument	**Measurements**	**Supplier**
LiCor 7500 IR gas analyser	Water Vapour [H_2O] CO_2	LiCor USA
TP3 Dew Point system	Air temperature and dewpoint	Meteolabor
BAT-Probe	wind, turbulence (50Hz), pitot-static, fluxes	ARA
FUST sensor	fast air temperature	ARA
PT100	air temperature	ARA
Eppley radiometers	solar and terrestrial radiation up- and down-welling	Eppley
Heimann KT15	IR surface temperature	Heimann
Riegl LD90	Laser altimeter for flying height and vegetation structure	Riegl
VegMeter	ndvi	ARA
OTS RT3003 INS/GPS	Position, altitude, attitude, accelerations (100Hz)	OTS